

A New Method for the C-Type Passive Filter Design

Abstract. The paper presents the new C-type high harmonic power filter design process whose aim is the reduction of total harmonic distortion in an industrial power supply system. A new method for C-type filter design is proposed and an example of the method application to an industrial plant is provided. The basis for the new algorithm is assuming, at the design phase, the required distribution of the harmonic current between the filter to be tuned to that harmonic and the supply network. This method takes into consideration the network equivalent impedance.

Streszczenie. Niniejszy artykuł przedstawia projektowanie energetycznego filtra typu C wyższych harmonicznych, którego zadaniem jest zmniejszenie współczynnika zawartości harmonicznych w przemysłowym systemie zasilania. Zaproponowano nową metodę projektowania C-filtru oraz przedstawiono przykład zastosowania tej metody projektowania w praktyce dla zakładu przemysłowego. (Nowa metoda projektowania filtra typu C).

Keywords: passive filter, compensation, power system harmonics, C-type filter.

Słowa kluczowe: filtry pasywne, kompensacja mocy biernej, harmoniczne, filtr typu C.

Introduction

An ever-increasing number of large-power nonlinear loads, installed in industry is the reason that passive harmonic filters are still the most common way to reduce voltage distortion at their points of connection. Many passive LC filter systems, of various structures and different operating characteristics have been developed [1] – [4]. Nevertheless, the single-tuned single branch filter still is the dominant solution for industrial applications, and it certainly is the basis for understanding more advanced filtering structures, such as the C-type filter.

An alternative solution can be active filters or hybrid filters that combine these structures [5] – [7]. Both the design and control of such systems can be a task employing artificial intelligence methods, e.g. neural networks or genetic algorithms [8] – [10].

The principal disadvantage of the majority of currently used filter-compensating device structures is poor filtering of high frequencies. In order to eliminate these disadvantages are usually used broadband (damped) filters of the first, second or third order; the C-type filter is included in the category of broadband filters. Broadband filters have additional advantage, substantial for their co-operation with power electronic converters: they damp commutation notches more effectively than single branch filters - they have a much broader bandwidth. They also more effectively eliminate interharmonic components (in sidebands adjacent to characteristic harmonics) generated by static frequency converters.

That filter, as compared to single branch filters, also ensures reduction of active power losses because the L_2C_2 branch (Fig. 1) is tuned to the fundamental harmonic frequency. The fundamental harmonic current is not passing through the resistor R_T , avoiding therefore large power losses.

The method for determining C-type filter parameters is described in [11]. Complex passive filters are more and more often designed using artificial intelligence methods, like genetic algorithms [12] – [13] that can also be effective in solving other problems [14] – [20].

Determination of the C-Type Filter Parameters

The paper describes a new method for determining the C-type filter parameters. Designing of filters for large power systems is a complex task: aside of determining the filter parameters to meet the design requirements, the filter shall be checked for possible resonance occurrences due to interaction with other passive components in the power system [21] – [22].

The filter parameters can be determined from relations given in [11]. This paper proposes a new, and simpler, method for determining the filter parameters. The method consists in assuming, at the design phase, the desired distribution of the harmonic current between the filter tuned to that harmonic and the supply network. This method requires taking into consideration the network equivalent impedance.

The C-type filter diagram is shown in Fig. 1.

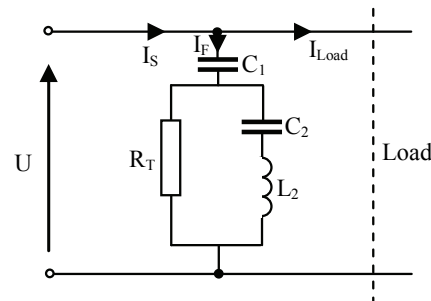


Fig. 1. The C-type filter circuit

The filter impedance is given by:

$$(1) \quad Z_F = \frac{\left(j\omega L_2 - j\frac{1}{\omega C_2} \right) R_T}{R_T + j\omega L_2 - j\frac{1}{\omega C_2}} - j\frac{1}{\omega C_1}$$

The L_2 and C_2 components are tuned to the fundamental frequency

$$(2) \quad L_2 = \frac{1}{\omega_1^2 C_2}$$

Hence

$$(3) \quad Z_F = \frac{jR_T(\omega^2 - \omega_1^2)}{R_T \omega \omega_1^2 C_2 + j(\omega^2 - \omega_1^2)} - j\frac{1}{\omega C_1}$$

The C-type filter is tuned to the resonance angular frequency $\omega_r = n_r \omega_1$

$$(4) \quad \omega_r = \sqrt{\frac{C_1 C_2}{L_2 \frac{C_1 + C_2}{C_1}}} \Rightarrow C_2 = C_1(n_r^2 - 1)$$

hence

$$(5) \quad Z_F = \frac{jR_T(\omega^2 - \omega_1^2)}{R_T\omega\omega_1^2 C_1(n_r^2 - 1) + j(\omega^2 - \omega_1^2)} - j\frac{1}{\omega C_1}$$

The filter reactive power (Q_F) for the fundamental harmonic is given by the relation:

$$(6) \quad Q_F = -\frac{U^2}{\text{Im}(Z_F(\omega_1))} \Rightarrow C_1 = \frac{Q_F}{\omega_1 U^2}$$

that is:

$$(7) \quad Z_F = \frac{jR_T U^2 (\omega^2 - \omega_1^2)}{R_T \omega \omega_1 Q_F (n_r^2 - 1) + jU^2 (\omega^2 - \omega_1^2)} - j\frac{\omega_1 U^2}{\omega Q_F}$$

Distribution of the load-generated harmonic current between the filter tuned to that harmonic and the system is:

$$(8) \quad \frac{I_S(n_r)}{I_F(n_r)} = k = \frac{|Z_F(n_r)|}{|Z_S(n_r)|} \Rightarrow R_T = \frac{U^2}{n_r^3 Q_F^2 k \omega_1 L_S} \sqrt{U^4 - n_r^4 Q_F^2 k^2 \omega_1^2 L_S^2}$$

Summarizing, the C-type filter parameters can be determined from formulas (6), (4), (2) and (8).

An Example of the C-Type Filter Design

In result of the arc furnace modernization (fig. 2.) its power and, consequently, the level of load-generated harmonics have increased. It was, therefore, decided to expand the existing reactive power compensation and harmonic mitigation system. Considering the system expansion the designed C-type filter should be tuned to the 2nd harmonic due to the fact that this harmonic, though present in the system, it is not reduced whereas the 3rd harmonic filters are already installed. Although currently the 2nd harmonic level in the existing system does not exceed the limit, connection of new loads may increase the 2nd harmonic to an unacceptable level.

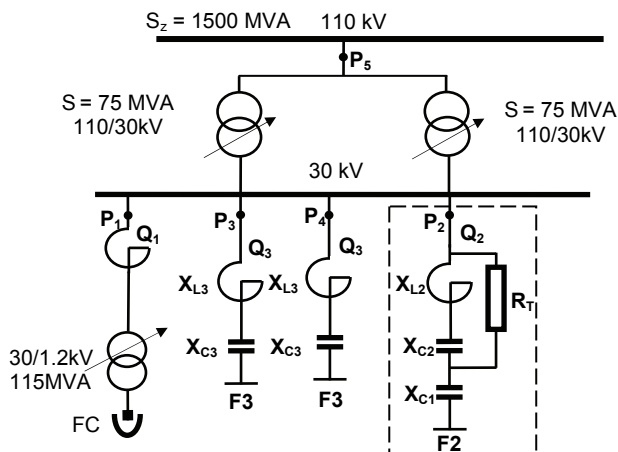


Fig. 2. Diagram of the modernized arc furnace power supply system

Prior to the modernization the system comprised two parallel, single-tuned 3rd harmonic filters that were the cause of a slight increase in the voltage 2nd harmonic. The increase in the arc furnace power entails an increase in the passive filters' powers. The planned extension of the system should also be taken into account. The increased power of the compensation circuit, as well as installation of

further filters, will increase the voltage 2nd harmonic level that will adversely affect the power system (table 1). Hence, it was decided to design an additional 2nd harmonic filter.

Table 1. Voltage harmonics (at the 30kV side) without filters and with two 3rd harmonic filters

Order voltage harmonic	Busbars voltage harmonics without filters	Busbars voltage harmonics with two 3rd harmonic filters
2.	1.76	2.47
3.	3.01	0.27
4.	1.66	0.95
5.	2.88	1.87
6.	1.12	0.78
7	1.75	1.24
8.	1.00	0.72
9.	1.12	0.81
THD	5.87	4.07

*Total harmonic voltage distortion factor THD_u determined from components up to 15th order.

For the arc furnace power supply system (Fig. 2) and the design requirements:

Network	3rd harmonic filters	C-type filter
$U = 30 \text{ kV}$ $S_z = 1500 \text{ MVA}$ $L_s = 3.129 \text{ mH}$ $R_s = 30.0 \text{ m}\Omega$	$Q_F = 20 \text{ Mvar}$ $L_3 = 18.48 \text{ mH}$ $C_3 = 63 \mu\text{F}$	$Q_F = 20 \text{ Mvar}$ $n_r = 1.9$ $q_{F2} = 10$ $k = 1$

the C-type filter parameters determined from (2), (4), (6) and (8) are: $C_1 = 70.736 \mu\text{F}$, $C_2 = 198.24 \mu\text{F}$, $L_2 = 51.11 \text{ mH}$, $R_T = 276.86 \Omega$.

Figure 3a shows frequency-impedance characteristics of: the power network, the resultant impedance of two single-tuned 3rd harmonic filters, and the C-type filter impedance. Figure 3b shows frequency-impedance characteristics of: the network, the resultant impedance of the network and two 3rd harmonic filters, and the resultant impedance of the network, two 3rd harmonic filters and the C-type filter.

Data listed in table 2 demonstrate that connecting the C-type filter results in the expected reduction of the 2nd voltage harmonic in the supply system, whereas other harmonics are reduced to a small extent. Further reduction of the second harmonic can be achieved by improving the C-type filter quality factor and, consequently, reduction of the filter impedance for the filter resonant frequency and increasing the impedance for higher harmonics.

Table 2. Voltage harmonics without filters, with two 3rd harmonic filters, and with two 3rd harmonic filters and the C-type filter

Order voltage harmonic	Busbars voltage harmonics without filters	Busbars voltage harmonics with two 3rd harmonic filters	Busbars voltage harmonics with two 3rd harmonic filters and the C-type filter
2.	1.76	2.47	1.32
3.	3.01	0.27	0.27
4.	1.66	0.95	0.91
5.	2.88	1.87	1.78
6.	1.12	0.78	0.74
7	1.75	1.24	1.18
8.	1.00	0.72	0.69
9.	1.12	0.81	0.78
THD _u *	5.87	4.07	3.37

*Total harmonic voltage distortion factor THD_u determined from components up to 15th order.

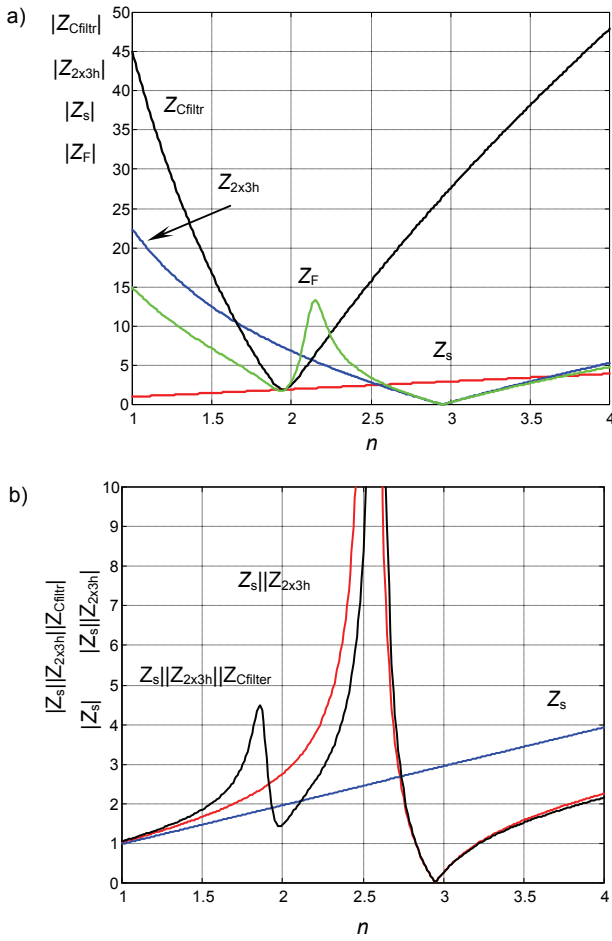


Fig. 3. Frequency-impedance characteristics of: a) the power network equivalent impedance (Z_s), the resultant impedance of two 3rd harmonic filters (Z_{2x3h}), the C-type filter impedance (Z_{Cfiltr}), the resultant impedance of two 3rd harmonic filters and the C-type filter (Z_F); b) the impedance seen from the load terminals: without filters (Z_s), the network equivalent impedance and two 3rd harmonic filters impedance connected in parallel ($Z_s||Z_{2x3h}$), and parallel connection of the network equivalent impedance, two 3rd harmonic filters and the C-type filter impedances ($Z_s||Z_{2x3h}||Z_{Cfiltr}$).

Figure 4a shows the C-type filter frequency characteristics for different quality factors, figure 4b illustrates the relation between the resistance R_T and the coefficient k that indicates the distribution of the current harmonic to which the filter is tuned.

Table 3. The percentage distribution of the harmonic current between the filter tuned to that harmonic and the supply network; the corresponding R_T values and the designed filter quality factor

I_F [%]	I_S [%]	k	R_T [Ω]
38.5	61.5	1.60	172
44.4	55.6	1.25	221
50.0	50.0	1.00	276.86
51.9	48.1	0.93	300
57.1	42.9	0.75	350
66.6	33.3	0.50	555
75.0	25.0	0.33	840
83.3	16.7	0.25	1111
91.0	9.0	0.10	2778

Data in table 3 shows the percentage distribution of the harmonic current between the filter tuned to that harmonic and the supply network. The values of the factor k corresponding to the R_T values are also provided in the table.

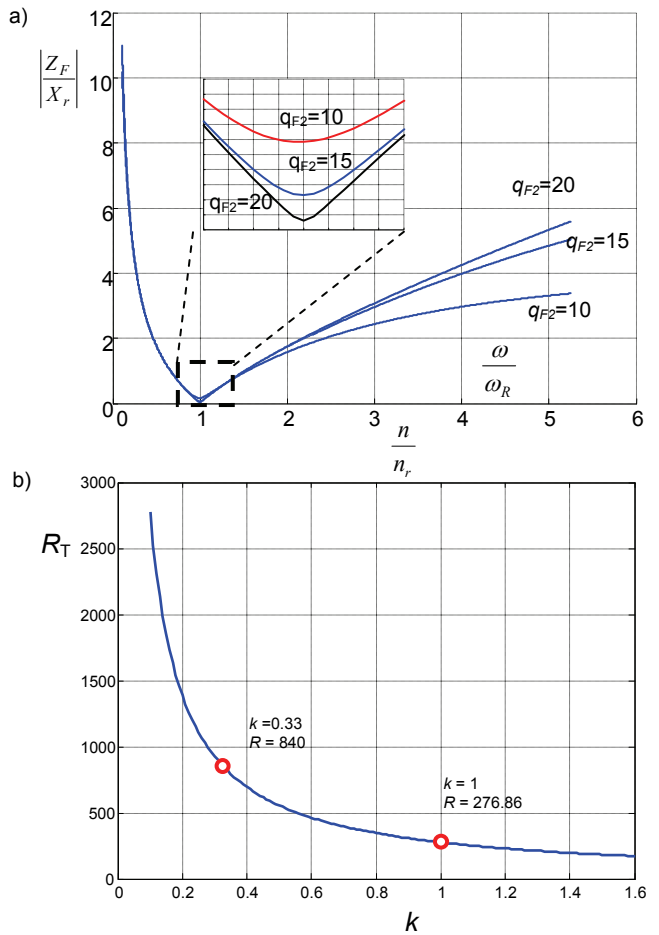


Fig. 4. a) The C-type filter frequency characteristics for various quality factors, b) the resistance R_T vs. the coefficient k

Implementation and Measurements

In order to verify the effectiveness of the proposed method has been designed a C-type filter for an electric arc furnace power supply system (Fig. 2).

The designed C-type filter was installed in the arc furnace supply system. The capacitance C_1 is composed of 60 capacitors (20 per phase) with capacitance $14.15\mu F$ each, which gives total capacitance $C_1 = 70.75\mu F$. The capacitance C_2 is composed of 24 capacitors (8 per phase) with capacitances $24.6\mu F$ each, which gives total capacitance $C_2 = 196.8\mu F$. The reactor L_2 parameters should be recalculated because of alteration of the capacitance C_2 due to the installation modifications ($L_2 = 51.48mH$). The resistor resistance is $R_T = 300\Omega \pm 10\%$. The diagram of the actual single-phase filter circuit is depicted in Fig. 5.

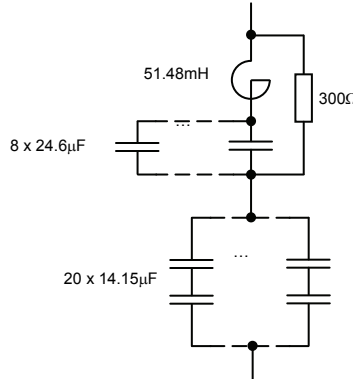


Fig. 5. Diagram of the actual C-type filter circuit

Measurements in the power system, configured according to the above specification, were carried out in order to check the correctness of the system operation. The instruments locations were: P_1 – arc furnace, P_2 – C-type filter, P_3 – first filter of 3rd harmonic, P_4 – second filter of 3rd harmonic, and P_5 – at the 110kV side. Essential results of measurements are tabulated in Table 4.

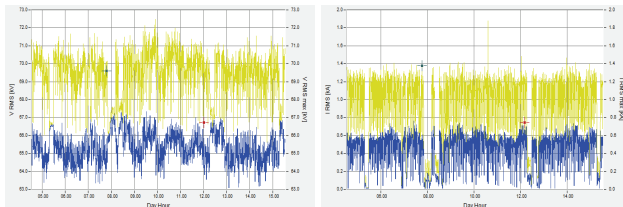


Fig. 6. The voltage and current at the 110kV side

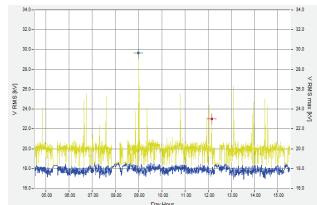


Fig. 7. The voltage at the 30kV side

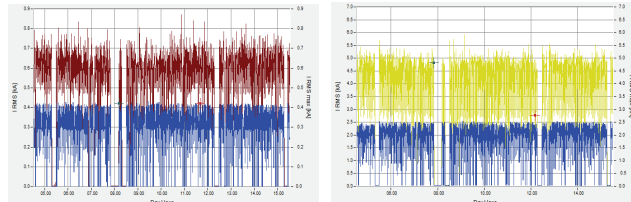


Fig. 8. The arc furnace and the C-type filter currents

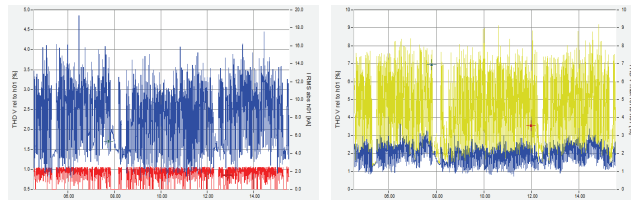


Fig. 9 Total harmonic voltage distortion factor THD_U at the 30kV and 110kV side

Table 4. The Measurement Results Obtained over a Period of 7 Days

Measurement point	P_1 Furnace	P_1 Furnace	P_2 Filter C	P_3 3rd harm. filter	P_4 3rd harm. filter	P_5 110kV	P_5 110kV
Furnace and filters in operation	No						No
U_{RMS} [kV]	18.29			17.59			65.04
I_{RMS} [A]	-	2383	391	398	385	602	86.5
P [MW]	-	93.75	0.083	0.234	0.198	105	12.14
Q [MVar]	-	71.19	19.55	19.84	19.68	28.2	6.52
S [MVA]	-	125.7	20.65	21.0	20.34	117.5	17.25
PF	-	0.744	0.0043	0.011	0.001	0.89	0.57
THD_U [%]	1.56			2.45			1.92
THD_I [%]	-	6.44	8.04	12.04	10.62	4.64	6.61
$I_{(1)}\text{RMS}$ [A]	-	2357	387	376	373	594	85.46
$U_{(1)}\text{RMS}$ [kV]	18.29			17.57			65.0
$U_{(2)}\text{RMS}$ [%]	0.06			0.73			0.42
$U_{(3)}\text{RMS}$ [%]	0.57			0.61			0.43
$U_{(4)}\text{RMS}$ [%]	0.04			0.34			0.19
$U_{(5)}\text{RMS}$ [%]	1.15			1.51			1.22
$I_{(2)}\text{RMS}$ [A]	-	58.7	32	10.8	9.8	15	2.21
$I_{(3)}\text{RMS}$ [A]	-	97.3	3.5	44.3	38.8	9	4.8
$I_{(4)}\text{RMS}$ [A]	-	23.1	1.5	5.1	4.5	3.7	0.6
$I_{(5)}\text{RMS}$ [A]	-	71.2	3.7	11.9	11.2	12.5	3.5
P_{st} [%]	1			16.66			9.17
							1.02

Figures 6 – 9 illustrate voltage and current waveforms recorded at the 110kV side (Fig. 6), the arc furnace supply voltage (Fig. 7), the arc furnace and the C-type filter currents (Fig. 8) and total harmonic voltage distortion factor THD_U at both: the 30kV and 110kV side (Fig. 9).

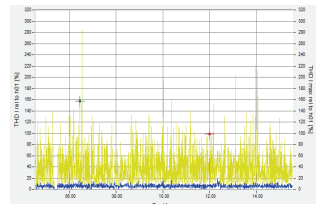


Fig. 10. Total harmonic current distortion factor THD_I at the 110kV side

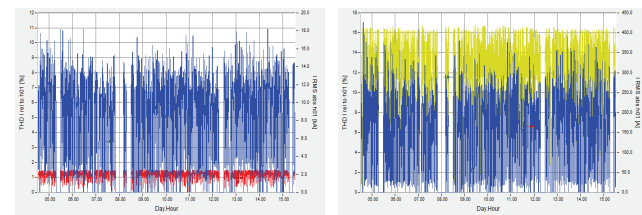


Fig. 11. Total harmonic distortion factor THD_I of the furnace and C-type filter currents

Figures 10 – 11 illustrate time plots of total harmonic current distortion factor THD_I at the 110kV side (Fig. 10) and harmonic distortion of the furnace and C-type filter currents (Fig. 11). Figure 12 shows the power system operating voltage spectrum (110kV and 30kV), figure 13 shows the 110kV side current spectrum and figure 14 shows spectra of the arc furnace current and the C-type filter current.

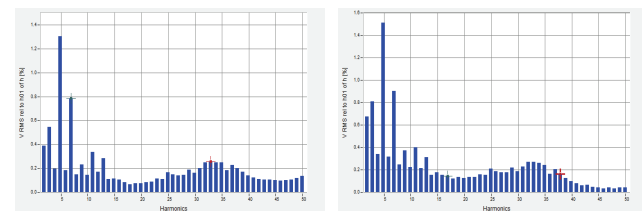


Fig. 12. Spectrum of the 110kV and 30kV side voltages

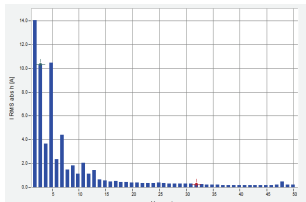


Fig. 13. The 110kV side current spectrum

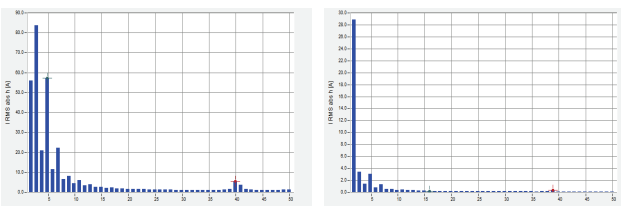


Fig. 14. Spectra of the arc furnace current and the C-type filter current

Conclusions

The measurements demonstrate that the C-type filter performance has met the requirements, i.e. it attains the expected reduction of reactive power, ensures the second harmonic reduction in the power system and harmonic distortion THD_U reduction by means of high harmonics mitigation. The measurements verified the proposed method and the C-type filter designed using this method operates according to the requirements. Figure 12 shows the power system operating voltage spectrum (110kV and 30kV), figure 13 shows the 110kV side current spectrum and figure 14 shows spectra of the arc furnace current and the C-type filter current.

Seemingly, the most advantageous solution is to increase the filter resistance R_T in order to ensure the largest possible part of the eliminated harmonic current flow through the filter instead of the supply network. But the increase in the resistance will reduce high harmonic currents through the filter. Thus a compromise between the filter ability to take over the harmonic the filter is tuned to, and its capability to mitigate other harmonics should be found. Increasing the R_T resistance makes the C-type filter frequency characteristic similar to that of a single-branch filter.

REFERENCES

- [1]. Nassif A. B., Xu W., Freitas W. An Investigation on the Selection of Filter Topologies for Passive Filter Applications, *IEEE Transactions On Power Delivery*, vol. 24, no. 3, July 2009.
- [2]. Kolar V., Kocman St. Filtracja harmonicznych w trakcyjnej podstacji transformatorowej, *Przegląd Elektrotechniczny* 12a/2011, 44-46
- [3]. Klempka R., Designing a group of single-branch filters, *Electrical Power Quality and Utilisation, EPQU'03*, September 17-19 2003, Krakow, Poland.
- [4]. Pasko M., Lange A. Kompensacja mocy biernej i filtracja wyższych harmonicznych za pomocą filtrów biernych LC, *Przegląd Elektrotechniczny* 04/2010, 126-129
- [5]. Rivas D., Morán L., Dixon J. W., Spinoza J. R., Improving Passive Filter Compensation Performance With Active Techniques, *IEEE Transactions On Industrial Electronics*, vol. 50, no. 1, February 2003.
- [6]. Salmerón P., Litrán S. P., Improvement of the Electric Power Quality Using Series Active and Shunt Passive Filters, *IEEE Transactions On Power Delivery*, vol. 25, no. 2, April 2010.
- [7]. Świątek B., Klempka R., Kosiorowski S., Minimization of the source current distortion in systems with single-phase active power filters and additional passive filter designed by genetic algorithms, *11th European Conference on Power Electronics and Applications, EPE2005*, September 11-14, 2005, Dresden.
- [8]. Świątek B., Hanelka Z., Neural Network-Based controller for an Active Power Filter, *10th International Power Electronics & Motion Control Conference EPE-PEMC 2002*, September 9-11, 2002, Cavtat & Dubrovnik, Croatia.
- [9]. Świątek B., Hanelka Z., A neural network-based controller for an active power filter. *14th International Power Quality Conf.* September 11-13, Rosemont, Illinois 2001.
- [10]. Świątek B., Hanelka Z., A single-phase active power filter with neural network-based controller, *IASTED International Conf. Power and Energy Systems*, July 3-6, 2001, Rhodes, Greece.
- [11]. Dugan R., McGranahan M., Electrical power systems quality, *McGraw-Hill*, 2002.
- [12]. Chang S.-J., Hou H.-S., Su Y.-K., Automated Passive Filter Synthesis Using a Novel Tree Representation and Genetic Programming, *IEEE Transactions On Evolutionary Computation*, vol. 10, No. 1, February 2006.
- [13]. Verma V., Singh B., Genetic-Algorithm-Based Design of Passive Filters for Offshore Applications, *IEEE Transactions On Industry Applications*, vol. 46, no. 4, July/August 2010.
- [14]. Chang G. W., Wang H.-L., Chu S.-Y., Strategic Placement and Sizing of Passive Filters in a Power System for Controlling Voltage Distortion, *IEEE Transactions On Power Delivery*, vol. 19, no. 3, July 2004.
- [15]. Younes M., Benhamida F. Hybrydowy algorytm genetyczny/mrórkowy jako metoda optymalizacji ekonomicznego rozsyłu energii, *Przegląd Elektrotechniczny* 10/2011, 369-372
- [16]. Eslami M., Shareef H., Mohamed A., Khajehzadeh M. Wykorzystanie algorytmu mrówkowego do równoczesnej kompensacji mocy biernej i stabilizacji systemu, *Przegląd Elektrotechniczny* 09a/2011, 343-347
- [17]. Gajer M., Zastosowanie algorytmów ewolucyjnych w obszarze badawczym Artificial Chemistry, *Przegląd Elektrotechniczny* 04/2011, 198-202,
- [18]. Eslami M., Shareef H., Mohamed A., Wykorzystanie technik sztucznej inteligencji przy projektowaniu systemów stabilizacji mocy systemu energetycznego, *Przegląd Elektrotechniczny* 04/2011, 188-197
- [19]. Sarac V., Cvetkovski G., Różne modele silnika oparte na zmiennosci parametrów przy zastosowaniu algorytmów genetycznych, *Przegląd Elektrotechniczny* 03/2011, 162-165
- [20]. Gajer M., Zastosowanie algorytmu ewolucyjnego do analizy nieliniowych obwodów elektrycznych, *Przegląd Elektrotechniczny* 07/2010, 342-345
- [21]. Badrzadeh B., Smith K. S., Wilson R. C., Designing Passive Harmonic Filters for an Aluminum Smelting Plant, *IEEE Transactions On Industry Applications*, vol. 47, no. 2, March/April 2011.
- [22]. Varetsky Y., Hanelka Z., Klempka R., Transformer energization impact on the filter performance, *8th International Conference on Electrical Power Quality and Utilisation*, September 21-23 2005, Cracow, Poland.

Autor

dr inż. Ryszard Klempka, Akademia Górnictwo-Hutnicza, Wydział Elektrotechniki, Automatyki, Informatyki i Elektroniki, al. Mickiewicza 30, 30-059 Kraków, e-mail: klempka@agh.edu.pl

The correspondence address is:
klempka@agh.edu.pl